TRACKING OF FUEL PARTICLES AFTER PIN FAILURE IN NOMINAL, LOSS-OF-FLOW AND SHUTDOWN CONDITIONS IN THE MYRRHA REACTOR

S. Buckingham[1], P. Planquart[1]
[1]: von Karman Institute, Chaussée de Waterloo 72, Rhode-St-Genèse, Belgium
sophia.buckingham@vki.ac.be; philippe.planquart@vki.ac.be;

K. Van Tichelen[2]
[2]: SCK•CEN, Boeretang 200, 2400 Mol, Belgium
kvtichel@SCKCEN.BE

ABSTRACT

This work on fuel dispersion aims at quantifying the design and safety of the MYRRHA nuclear reactor. A number of situations with possible release of a secondary phase into the primary coolant loop are investigated. Among these scenarios, an incident leading to the failure of one or more of the fuel pins is simulated while the reactor is operating in nominal conditions, but also in natural convection regime either during accident transients such as loss-of-flow or during the normal shut-down of the reactor.
Two single-phase CFD models of the MYRRHA reactor are constructed in ANSYS Fluent to represent the reactor in nominal and natural convection conditions. An Euler-Lagrange approach with one-way coupling is used for the flow and particle tracking. Firstly, a steady state RANS solution is obtained for each of the three conditions. Secondly, the particles are released downstream from the core outlet and particle distributions are provided over the coolant circuit. Their size and density are defined such that test cases represent potential extremes that may occur. Analysis of the results highlights different particle behaviors, depending essentially on gravity forces and kinematic effects. Statistical distributions highlight potential accumulation regions that may form at the free-surfaces, on top of the upper diaphragm plate or at the bottom of the vessel. These results help to localize regions of fuel accumulation in order to provide insight for development of strategies for accident mitigation.

KEYWORDS
Fuel dispersion, MYRRHA reactor, CFD, Lagrangian tracking

1. INTRODUCTION

This work is part of the MYRRHA project [1] founded by SCK•CEN and aims at simulating with a CFD model the primary coolant loop of the MYRRHA reactor. The MYRRHA reactor is a flexible fast spectrum research reactor that is conceived as an accelerator driven system (ADS), cooled by liquid Lead-Bismuth Eutectic (LBE). In the design version 1.4 selected for the study, a pool-type system was selected in which all the components of the primary loop (pumps, heat exchangers, fuel handling tools, experimental rigs, etc.) are inserted from the top into the LBE pool. A detailed description of the loop will be proposed while describing the general flow patterns.
Most of the reactor's mechanical components are designed to operate in single-phase flow regime, thus the presence of a secondary phase may have damaging effects. In this context, a thorough safety assessment of the facility is required covering a number of accidents. Among these scenarios, an incident leading to the failure of one or more of the fuel pins would result in the release of fuel products directly

into the coolant. Among the threats are core damage, criticality effects related to fuel accumulation and coolability effects due to potential blockage and local heat flux increase.
Two steady-state models of the reactor in nominal and natural convection conditions are used to transport the fuel particles over the coolant circuit. The methodology described hereafter briefly reviews the approach used to construct these CFD models. The different numerical models selected to perform these simulations are then introduced. Particle characterization is explained along with a choice of dispersion cases to simulate. Finally, an analysis of statistical distributions obtained for extreme cases is proposed.

2. METHODOLOGY

2.1. Single phase steady state models

2.1.1. Nominal conditions

A CFD model of the MYRRHA reactor version 1.4 operating in nominal conditions is first constructed. A mesh of 9.5 million cells is generated with snappyHexMesh. This single phase, steady, turbulent and incompressible flow simulation run with ANSYS Fluent is described in detail in [2].
To correctly simulate the transport of fuel products it is essential to accurately compute the background flow field. Therefore, the first objective is to obtain a comprehensive description of the entire pool by constructing a steady-state model that includes all the necessary physical modelling. Due to a large range of scales and the diversity of the physical phenomena involved, several simplifications and modeling assumptions have been made. A homogeneous representation is used in the more complex parts where porosity is adjusted to match the expected pressure drops. The rotating component of both pumps is replaced by a momentum source that imposes flow motion over the closed-loop. The axial and tangential components are adjusted to match the nominal mass flow rate of 9440 kg/s and an average swirl angle of 27° respectively. The free-surfaces are approximated as free slip boundaries, since at steady state, pressure is approximately uniform on the surfaces. The nuclear reaction in the core can be approximated by a radial heat source distribution of 100 MW. An additional 2 MW is distributed in the in-vessel fuel storages, IVFS, while the heat is extracted by applying a heat sink in the heat exchangers, HX, dependent on the convective exchange between the LBE and the water tubes and defined as:

$$S_{HX} = UA(T - T_{water})/V_{HX} \qquad (1)$$

where A is the exchange surface of the HX tubes, V_{HX} is the HX volume, T_{water} is fixed to 200 °C and U is the total local heat transfer (ref. [2]). Conjugate Heat Transfer, CHT, through the main walls that are subjected to strong temperature gradients is taken into account.

2.1.2. Natural convection regime

As introduced previously, fuel dispersion occurring in the event of a pin failure may also take place in a natural convection regime, which may appear during both accident transients as well as during the normal shutdown of the reactor. For instance, in the event of a loss of flow (pump failure or loss of power of the pumps), the reactor will be stopped by the insertion of the safety rods. A natural circulation flow will establish driven by the decay heat. It will therefore continue operating in very different conditions than during nominal operation. Naturally, fuel particles from pin failure will behave differently as they will be exposed to a very different flow field.
To account for this flow regime, a second single-phase CFD model is constructed to investigate the natural convection regime. First, to evaluate the case driven by the decay heat power of the core, two power levels are chosen: at 3 % and 1 % of the nominal core power, CP, which may occur at roughly 120 s and 9200 s respectively after the insertion of the safety rods. The first case at 3 % CP is representative

for the loss of flow, where the pumps fail and provoke the safety rod insertion by the reactor protection system. The second case at 1 % CP is representative for a normal reactor shutdown condition where the pumps are stopped manually after an initial forced cooling time. At those two instants, the LBE free-surface levels are assumed to have reached an equilibrium level. A corresponding CAD model of the reactor is used to generate a new mesh and a similar set-up as the one used in nominal conditions is implemented. The porosities and resistances remain unchanged except for the pump. These are adjusted to represent the correct blockage of the flow path and corresponding pressure losses in the range of expected flow rates. The total heat source in the IVFS is kept equal to the maximum of 2 MW at 3 % CP as an enveloping value. At 1 % CP, it is set to the enveloping decay heat of the spent fuel equal to 120.7 kW.

2.2. Lagrangian tracking of the particles

The Euler-Lagrange approach is used as general methodology to investigate fuel dispersion in the primary loop. A detailed description of the modeling can be found in [3] but a short summary is proposed here.
The flow solution obtained in either forced or natural convection regime is used as initial field. The fuel is then injected and its redistribution over the reactor pool is simulated. The fluid phase and the solid fuel particles are treated in an Eulerian and a Lagrangian frame respectively. Therefore the particle trajectories are predicted by solving the equation of motion that integrates the force balance on each particle, taking into account: weight, buoyancy, pressure gradient, drag, lift and virtual mass. A turbulent dispersion model (DRW) is used to generate fluctuating velocities and account for dispersion of the particles due to turbulence. The flow is considered to be dilute enough to adopt a one-way coupling approach, where the dispersed phase is affected by the carrier phase but not vice-versa. This assumption results in a considerable gain in computational time since the LBE flow solution remains unchanged.

2.3. Definition of accident scenarios

The particles are characterized in order to be representative of the possible range of accident scenarios in terms of density and particle sizes. The fuel is made of 30% Pu MOx that defines the theoretical density (TD) as a function of temperature. The density of the released particles at the injection depends on the burn-up reached at the time of dispersion. The range of probable density values has been identified as being [60-95] % of TD [4]. The temperature dependent properties of LBE are taken from the LBE handbook [5], different cases are illustrated in Fig. 1 a). The solid particles are assumed to be spherical in shape and the range of diameters under consideration is [0.125-3.155] mm. The lower bound is fixed to the diameter below which particles are dragged along with the flow while the upper bound is the largest diameter that fits between the fuel pins.
The particle temperature is taken equal to the local LBE temperature to which 5 K is added to account for heat generated by the fuel particle itself. Only the four extreme cases, listed in Table I, are simulated here. Across the temperature range present in the reactor, it is only for a density equal to 95% of TD that the particle is denser than LBE.

Table I. Fuel dispersion test cases

Case number	1	2	3	4
Particle density	60 % TD	60 % TD	95 % TD	95 % TD
Particle diameter	3.155 mm	0.125 mm	0.125 mm	3.155 mm

The particles are released from an injection point located at the centre of the outlet of the core support plate, at (x, y, z) = (0, 0.8, 0). The number of injected particles needs to be large enough to include the random effects of turbulence. A sensitivity study has been performed in test case 2, and distributions

shown in Fig. 1 b) demonstrated that 1000 particles is sufficient to insure convergence of the final particle distribution.

For the computational time to remain reasonable, the tracking time in forced convection is limited to 812 s which is equal to twice the characteristic time of the reactor loop ($\bar{t} = V/Q_v$), where V is the volume and Q_v its volumetric flow rate. In natural convection, the tracking time is increased to 3500 s. To extend the analysis to larger time scales, probable evolution of the particles repartition or possible asymptotic behavior is examined case by case.

As for boundary conditions, in nominal operation the tracking is stopped when the particles re-enter the core after completing a loop around the primary circuit. Their final position is therefore taken at the core inlet height. At the contrary, in natural convection the particles can pass through the core since the densest particles may drop down into the core region. Therefore, the previous boundary condition is no longer used and a continuous tracking method is applied.

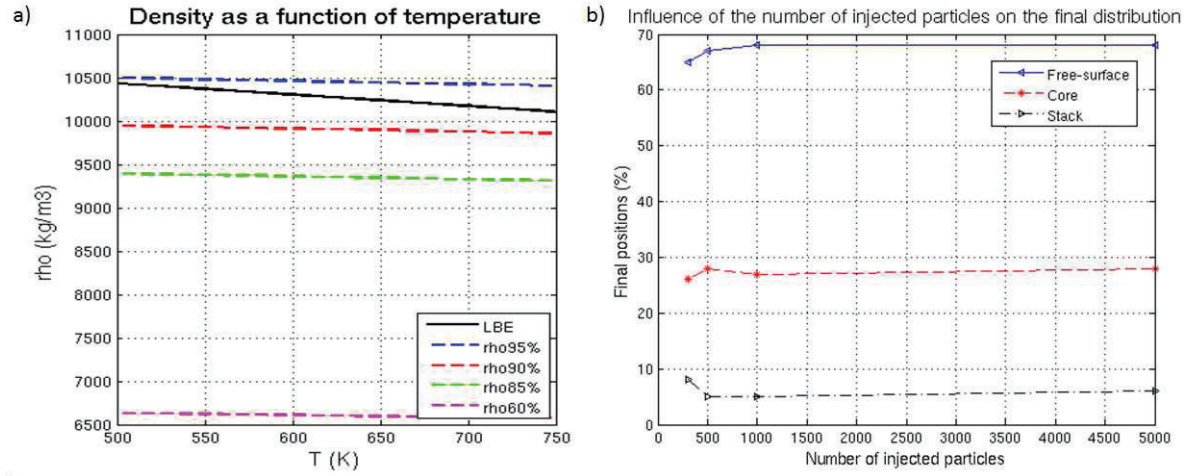

Figure 1. a) Temperature dependence of the particle density b) Influence of the number of injected particles on the final distribution – test case 2

3. PRESENTATION OF THE RESULTS

3.1. Thermal-hydraulic flow fields

3.1.1. Nominal conditions

Velocity contours obtained along the two vertical symmetry planes are shown in Fig. 2 a). The levels are given up to 1 m/s and saturated above. The nominal mass flow rate leads to a maximum velocity of 2.37 m/s in the pumps. The two pump jets first impact the bottom of the vessel before colliding in the centre of the reactor leading to a characteristic layer of upward flow directed towards the core. In addition, for each pump two large recirculation bubbles are created in the lower plenum, LP. Subsequently, the flow is distributed through the different core rings after which the different jets tend to merge in the plane of the two pumps. This behavior is mainly caused by the descending flow motion that appears in this same plane (ref. Fig. 2 b)). Indeed, once the flow reaches the free-surface, part of it exits through the last row of barrel holes but a large portion goes back down into the barrel before exiting through the other rows of holes lower down. Finally, the flow in the upper plenum, UP, goes back into the HX.

The various heat sources and sinks result in substantial temperature variations throughout the reactor. Static temperature contours in the vertical symmetry plane (x,y) are shown in Fig. 3 a).

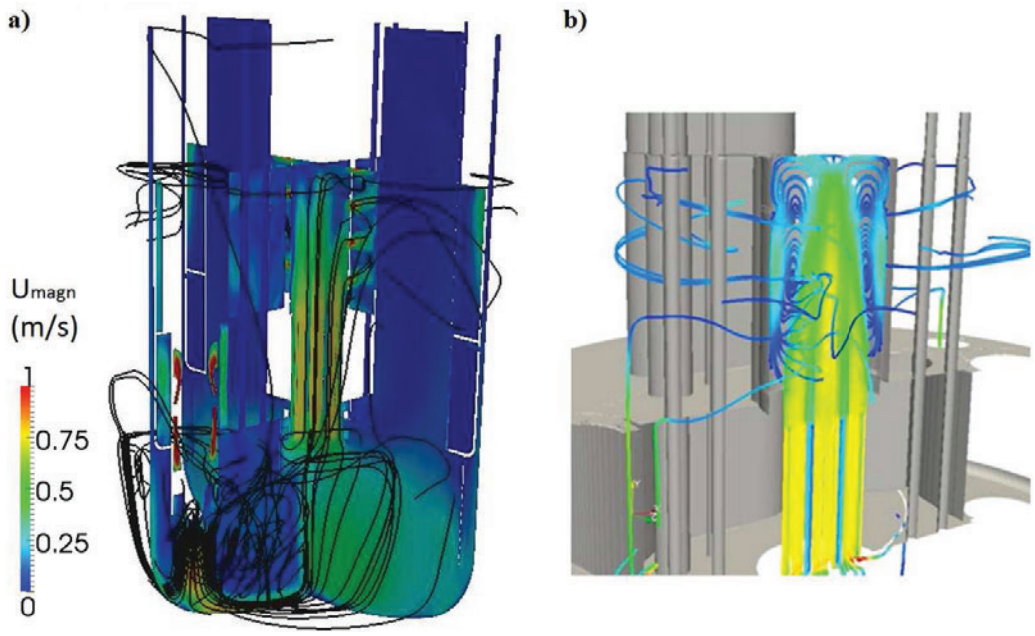

Figure 2. a) Velocity contours and streamlines b) Streamlines in the barrel region

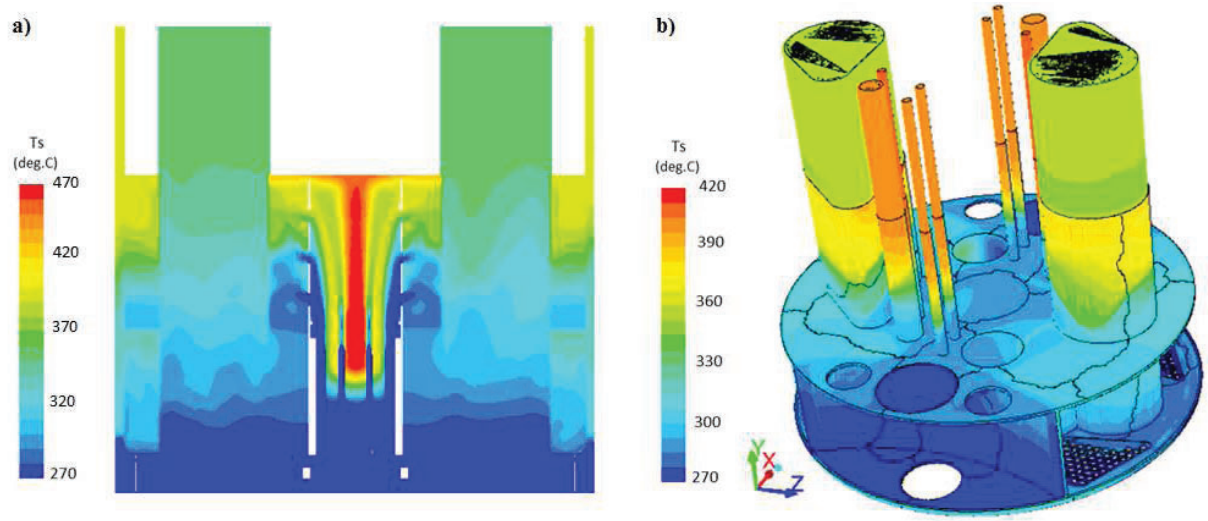

Figure 3. Temperatures in nominal conditions a) Field values along plane (x,y) b) Wall values

A maximum temperature of 471 °C is reached in the core. The mass flow average core inlet and outlet temperatures correspond to 272 °C and 344.5 °C respectively, in agreement with an injected power of 100 MW ($P = \dot{m}C_p\Delta T$). The effect of modeling CHT through the solids clearly appears, as the LBE is heated by conduction through the walls. Wall temperatures are seen in Fig. 3 b), where the strongest gradients appear at mid-height along the In-Vessel Fuel Handling Machine (IVFHM), in the region located in the UP. These thermal stresses are a major concern for the structural design of the reactor.

3.1.2. Natural convection regime

Due to inherent flow unsteadiness present in the natural convection regime, numerical convergence is mainly assessed based on flow quantities at several locations in the reactor. Although numerical instabilities are unavoidable with the current steady approach, these are limited to an acceptable level and

a satisfactory convergence is reached. In particular, the total mass flow rate through the core stabilizes to a value of 370 kg/s at 3 % CP, which represents 3.9 % of the nominal mass flow rate. At 1 % CP, this value reduces down to 195 kg/s which represents 2.1 % of the nominal value. As in forced convection, heat is removed by convective exchange with the use of a heat sink (ref. Eq. 1).

Velocity contours in the symmetry plane (x,y) are shown in Fig. 4. At 3 % CP, velocities as high as 17 cm/s are reached in the core, while these are limited to [10-14] cm/s at the exit of the pumps. Flow jets around [5-10] cm/s appear through the barrel holes, but elsewhere in the pool areas velocities remain below 5 cm/s. Naturally, the velocities further decrease at 1 % CP along with the buoyancy effects, with a maximum velocity of 10 cm/s above the core and levels that remain below 3 cm/s elsewhere.

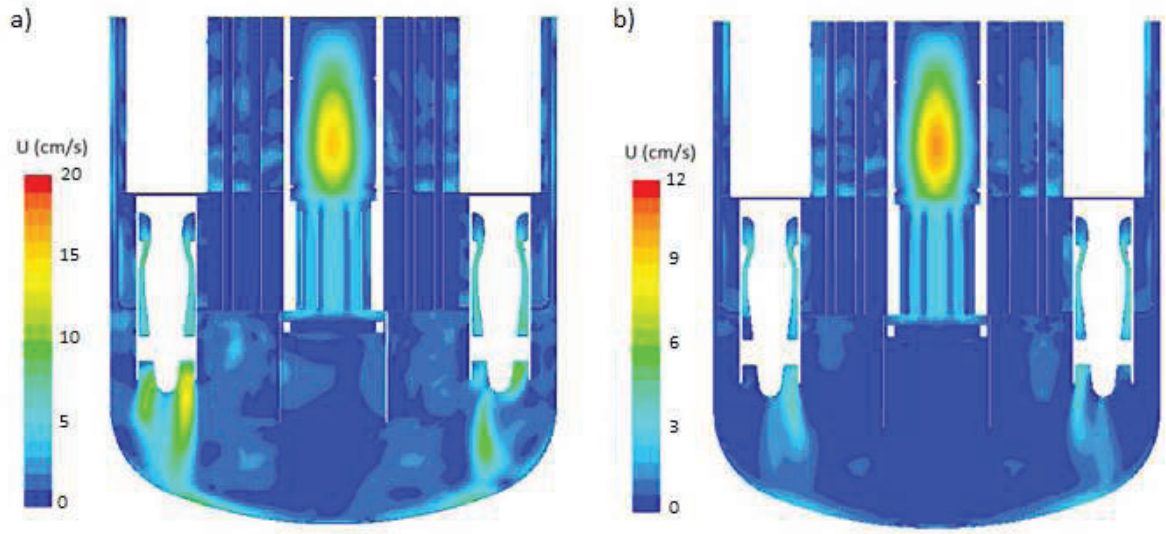

Figure 4. Velocity contours in the vertical symmetry plane (x, y) a) 3 % CP b) 1 % CP

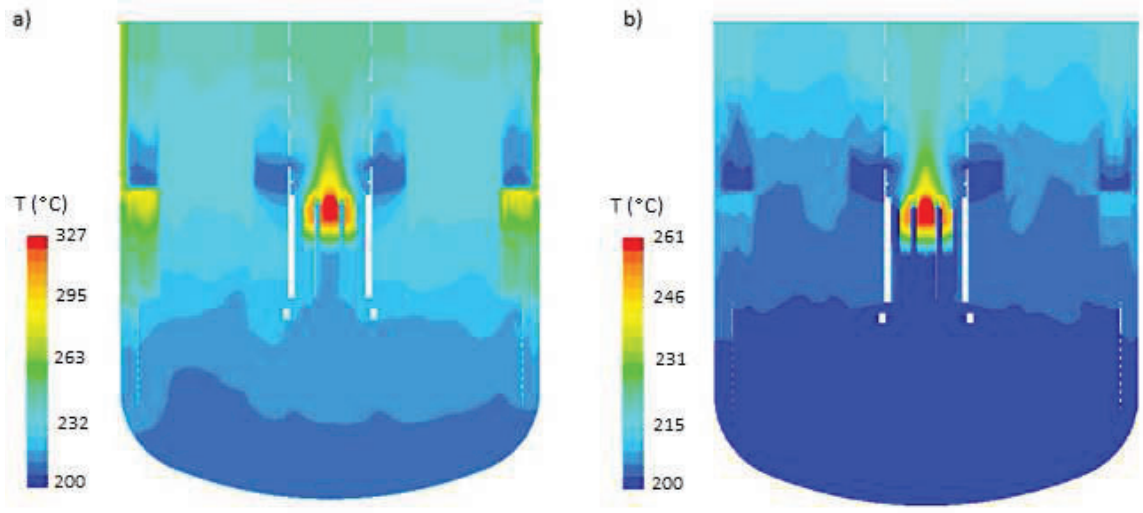

Figure 5. Temperature contours in the vertical symmetry plane (x, y) a) 3 % CP b) 1 % CP

Temperature contours are given in Fig. 5. At 3 % CP, a maximum temperature of 323 °C appears in the core center, while a minimum value of 200 °C is observed along the HX; however the flow exits into the LP at an average temperature of 206 °C. Stratification establishes in the UP going from 206 °C to 251 °C,

therefore exhibiting a temperature gradient of 45 °C. Such low temperatures are reached due to outflow through the inlets of the HX.

At 1 % CP, the maximum temperature in the core reduces to 261 °C. As for the previous scenario representative of a loss of flow, reversed flow through the HX inlets causes cold LBE as low as 206 °C to flow back into the UP, inducing a temperature gradient of 16 °C in this area of the reactor. In this case, the heat coming from the IVFS by conduction through the inner vessel is very much reduced.

3.2. Fuel dispersion

3.2.1. Nominal conditions

Case 1: d = 3.155 mm, ρ = 60 % TD

In this first case, the largest and lightest particles are released at $t = 0$ s. The final particle distribution indicates that 100 % of the particles are located at the free-surface level after 812 s. Particle trajectories colored with residence time are illustrated in Fig. 6.

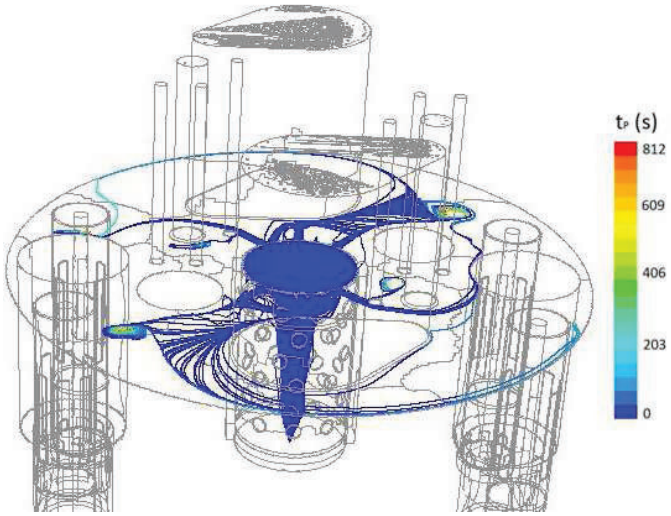

Figure 6. Case 1 - Particle trajectories colored with residence time

These show that particles are pushed straight to the free-surface, without even exiting through the barrel holes, because of strong buoyancy forces. Indeed, this accident scenario is characterized by the strongest buoyancy forces as particles are the largest and least dense compared to LBE. Final particle positions are represented by light blue dots viewed at free-surface height from the top of the reactor in Fig. 7 a).

The positions indicate that particles accumulate mainly in the two large recirculation areas caused by the barrel jets impacting on the Si-doping tubes, visible in Fig. 7 b). Mitigation strategies should therefore be developed to handle these areas of free-surface accumulation.

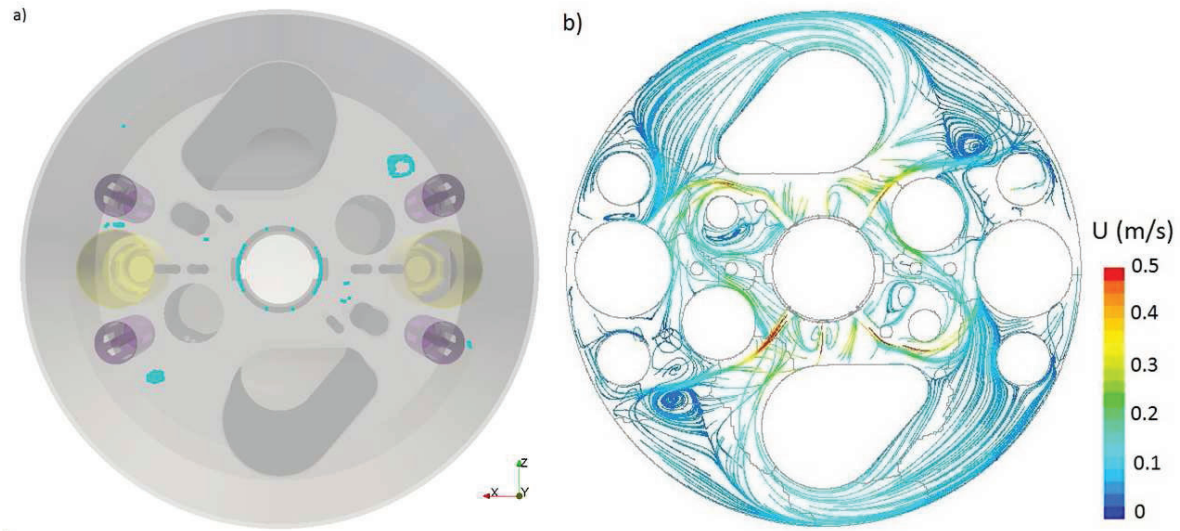

Figure 7. Case 1 – Nominal flow a) Final particle positions b) Flow streamlines

Case 2: d = 0.125 mm, ρ = 60 % TD

Unlike the previous case, not all but only 67 % of the particles remain at the free-surface, while 27 % re-enter the core and the remaining 5 % are still circulating. During the simulation, 80 % have reached the free-surface level, which implies that 13 % have gotten re-entrained back into the UP. To understand what could be the role of turbulent dispersion in this behavior, the case is re-run without taking these effects into account, resulting in 100 % of the particles reaching the free-surface and remaining there. This confirms that the weaker buoyancy forces (reduced particle size) still are important but turbulent dispersion effects, which are responsible for re-entraining some of the particles from the free-surface, cannot be neglected.
Naturally, particles that remain at the free-surface level accumulate in the exact same areas where flow recirculations appear. As for the particles re-entering the core, these are quite uniformly distributed over the inlet section. The risk of core blockage is limited since the particles are small in size, therefore similarly to case 1, only the free-surface accumulations remain to be addressed. At a larger time scale, one can expect that eventually all particles will get re-entrained from the free-surface and re-enter the core.

Case 3: d = 0.125 mm, ρ = 95 % TD

As indicated by Fig. 1 a), this case is characterized by particles that are denser than the LBE flow. To describe the behavior of the particles, the Stokes number can be computed as: $St = \tau_P/t$. This number represents the ratio between the characteristic time t of the flow and the relaxation time of the particle, τ_P, defined as:

$$\tau_P = \frac{\rho_p}{\rho_f}\frac{4d_p^2}{3C_D Re_p \upsilon_f} \qquad (2)$$

For a characteristic velocity of 0.5 m/s and length scale of 1 m, a particle Reynolds number, Re_p, of about 10, this yields: St << 1. Consequently, a majority of the particles are expected to follow the flow. Indeed, the final particle distribution indicates that 78 % re-enter the core, 6 % are still circulating and 16 % remain at the free-surface in the same recirculation areas than observed in test case 1. Indeed, the strong disturbances created by the barrel jets induce upward velocities of about 5 cm/s in these recirculation areas. These generate an upward kinetic force that is sufficient to maintain the particles at the free-surface. Final particle positions are represented in Fig. 8 a). These appear to be maintained by upward

velocities of about 0.05 m/s which result in kinetic forces that are comparable to the gravity forces acting in the opposite direction.

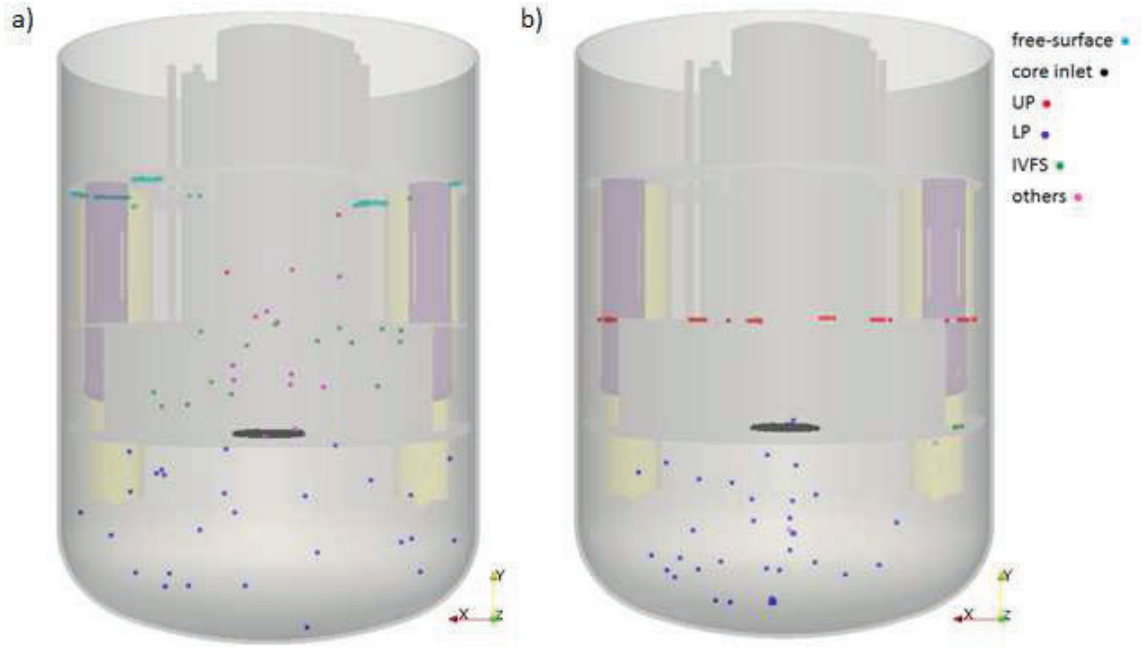

Figure 8. Final particle positions – Nominal flow a) Case 3 b) Case 4

To conclude, the only potential threat in this case would be core blockage, which is limited due to small particle size. Once again, an asymptotic behavior is expected where particles will slowly keep re-entering the core.

Case 4: d = 3.155 mm, ρ = 95 % TD

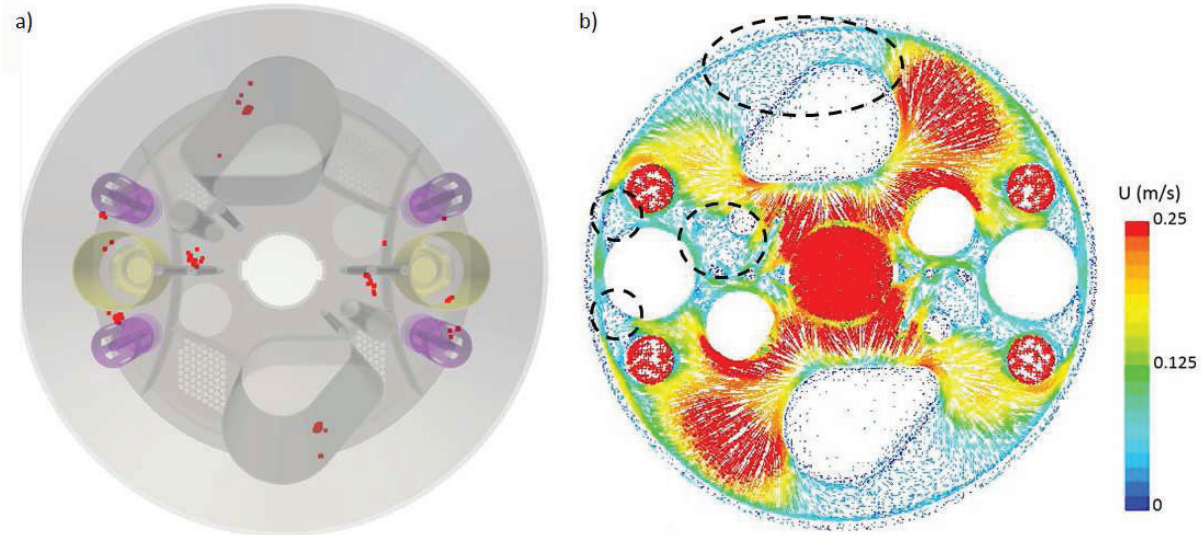

Figure 9. Case 4 – Nominal flow a) Final particle positions on top of upper diaphragm plate b) Velocity vectors 2 cm above upper diaphragm plate

As a preliminary analysis already suggests (St ~ 0.1), this scenario exhibits the heaviest particles and therefore flow effects no longer dominate. Under the effect of strong gravity forces, a large proportion of particles, 56 %, fall straight down onto the upper diaphragm plate. These clearly appear in Fig. 8. b), as a layer of red particles deposits on top of the plate. There are still 20 % that follow the flow back to the core while the rest remains circulating in the LP. Preferential areas of particle deposit appear on the top view proposed in Fig. 9 a). These specific areas are essentially located in between the pumps and HX, as well as behind the IVFHM. They can be associated to regions of low velocities as observed in Fig. 9 b).
To conclude, this last test case exhibits a risk related to these localized accumulations. In particular, the effect of heat flux from particles to the diaphragm should be analyzed, especially considering that the particle deposit is expected to keep growing in time.

3.2.2. Natural convection regime

Case 1: d = 3.155 mm, ρ = 60 % TD

As in forced convection, this case is characterized by strong upward buoyancy forces that push the particles to the free-surface. Similarly, an asymptotic behavior has been reached where almost all particles have accumulated at the free-surface level after 812 s, with 97.5 % and 98.5 % for 3 % and 1 % of CP respectively.

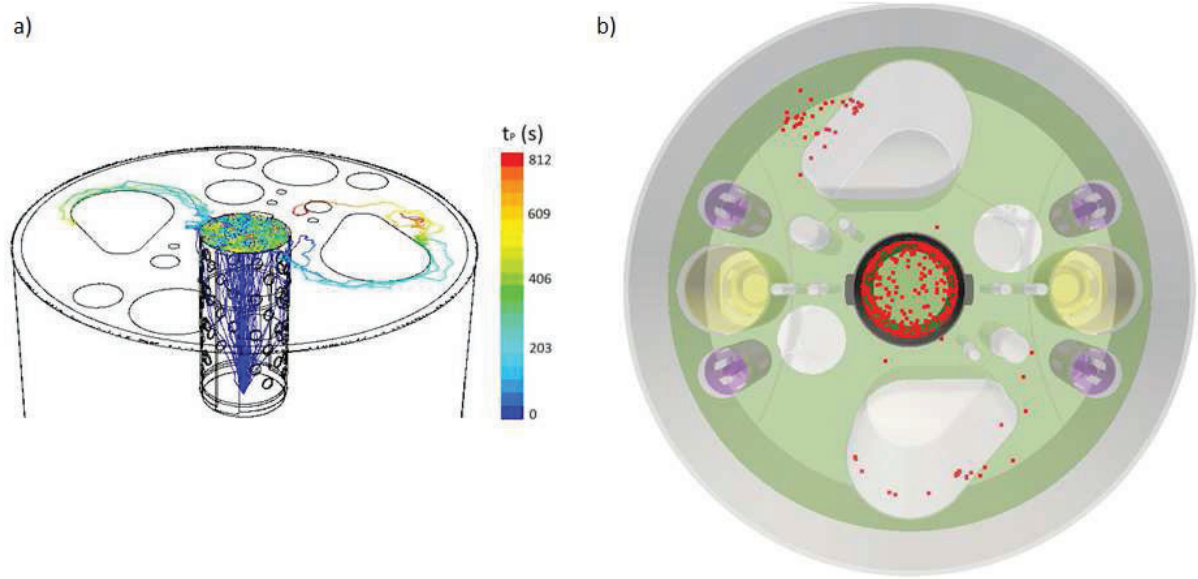

Figure 10. Case 1 at 3 % CP a) Particle trajectories colored with particle residence time b) Particle final positions at free-surface level

However, previously in nominal conditions, the particles reaching the free-surface were then free to exit straight into the UP since the free-surface level was intersecting with a row of barrel holes. In natural convection, the free-surface that has equilibrated to a different level is higher and lies in between two rows of barrel holes such that a majority of the particles remain stuck inside the barrel, as shown in Fig. 10 b).
To conclude, this test case illustrates how sensitive the results can be with respect to the free-surface behavior. The free-surface height, that remains fixed in this single-phase modeling approach, can have a significant influence on particle accumulation regions at the free-surface. A multiphase approach with interface tracking could be a considerable added value by providing a more accurate modeling of the free-

surface behavior. Also it shows the importance of changing the pattern of holes in the barrel as to have openings to the UP at each level.

Case 2: d = 0.125 mm, ρ = 60 % TD

In natural convection, reversed flow is observed through the first two rows of barrel holes as shown in Fig. 11. After re-entering the barrel, the flow goes down along the inside walls, below the injection point (red circle) before going back-up. Regardless of the tracking time, final distributions indicate that all particles accumulate at the free-surface as shown in Fig. 12 a).

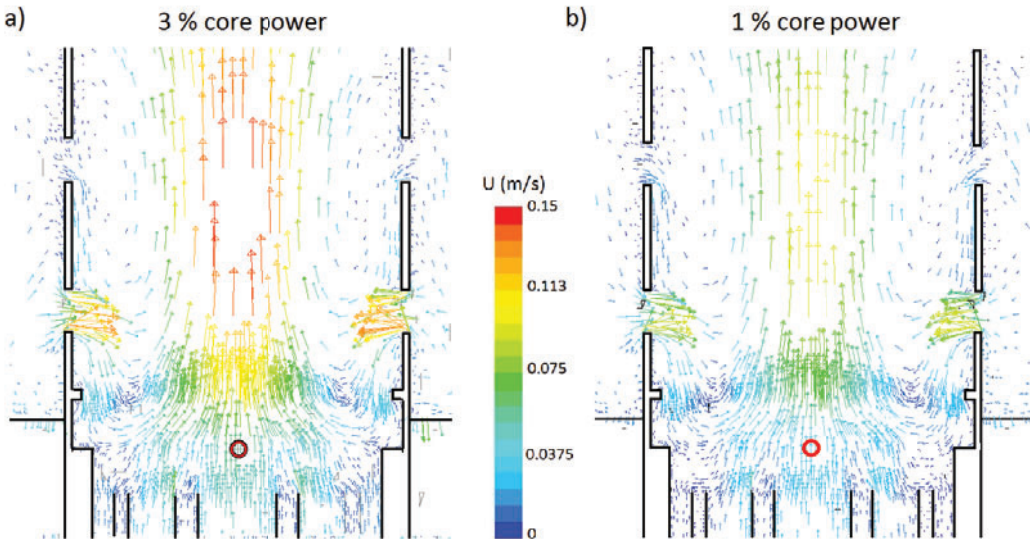

Figure 11. Velocity vectors in barrel region (vertical symmetry plane x=0) a) 3 % CP b) 1 % CP

As opposed to case 1 where a majority of the particles remained trapped inside the barrel, in this case most of them exit into the UP. Indeed, buoyancy forces are reduced and more particles are able to follow the outflow. Naturally, particles mainly accumulate in the two large recirculation areas behind the IVFHM as indicated in Fig. 12 b).

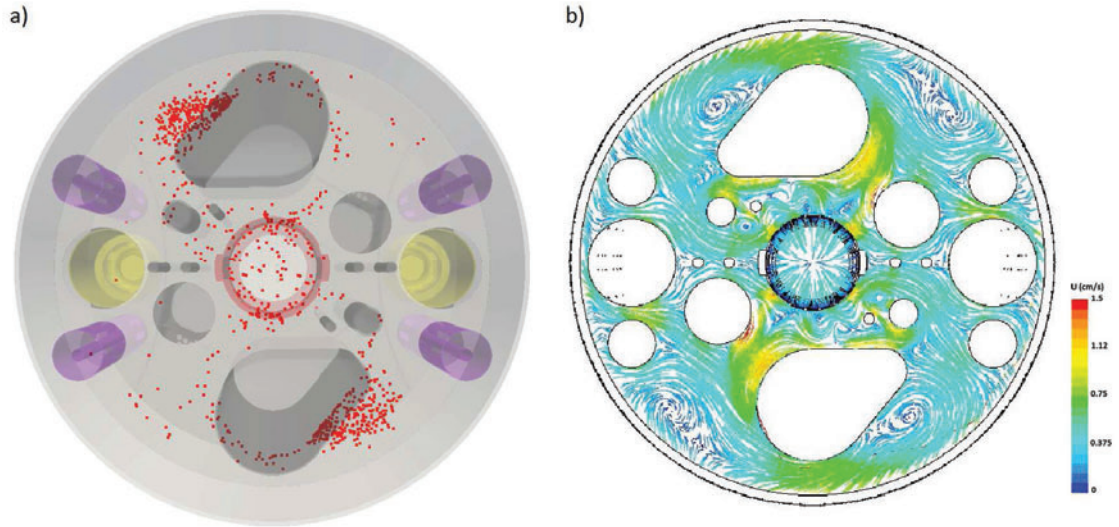

Figure 12. Case 2 - 3 % CP a) Final particle positions b) Flow streamlines at free-surface level

Case 3: d = 0.125 mm, ρ = 95 % TD

Final particle positions and particle distributions are given with corresponding colors in Fig. 13 a) and b) respectively. After 3500 s, a small deposit (16-17%) forms on top of the diaphragm (DIA.) plate. A larger proportion of particles has already passed to the LP at 3 % CP compared to 1 % CP since the flow is more energetic. For similar reasons, a small amount of particles is found in the bottom of the vessel at 1 %, while at 3 % all particles remain circulating in the LP

a)

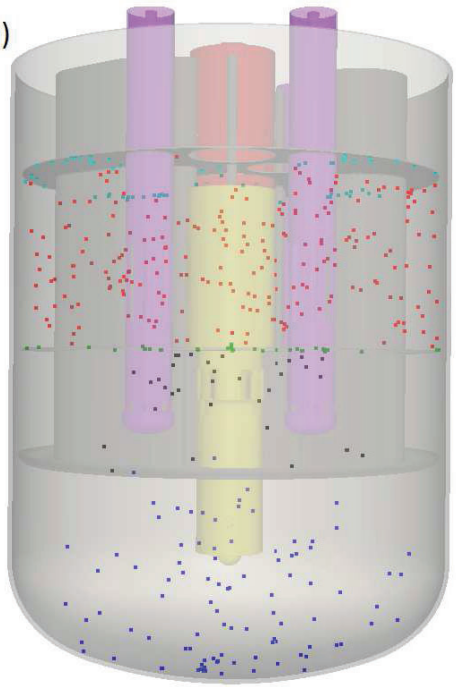

b) Particle distributions at t=3500s

Scenario	3 %	1 %
Free-surf.	5 %	12 %
DIA.	16 %	17 %
Pump box	12 %	7 %
UP	30 %	44 %
LP	33 %	19 %
Other	4 %	-

Figure 13. Case 3 – Continuous tracking a) Final positions b) Particle distributions at 3500 s

Case 4: d = 3.155 mm, ρ = 95 % TD

In forced convection, the flow above the core from where the particles are released is strong enough to entrain them upwards into the UP. In natural convection however, the flow is much less energetic and a large amount of particles is expected to drop down into the core region. For this reason, continuous tracking is applied and resulting particle distributions are given in Table II.

Table II. Case 4 in natural convection – Particle distributions with continuous tracking

Reactor region	Core	Top DIA.	UP	LP
3 % CP	8 %	79 %	7 %	6 %
1 % CP	15 %	28 %	5 %	52 %

Together with final particle positions shown in Fig. 14, these results indicate that in this case the dispersion strongly depends on the CP. At 3 % CP, the flow is strong enough for a majority of the particles to pass into the UP. Eventually, 79 % fall on top of the upper diaphragm plate, while only 6 % drop in the bottom of the reactor vessel. On the contrary, at 1 % CP a lot less particles get entrained upwards, and only 28 % end-up falling on the top diaphragm plate. A large amount goes back down into the core, and 52 % fall down to the bottom of the vessel.

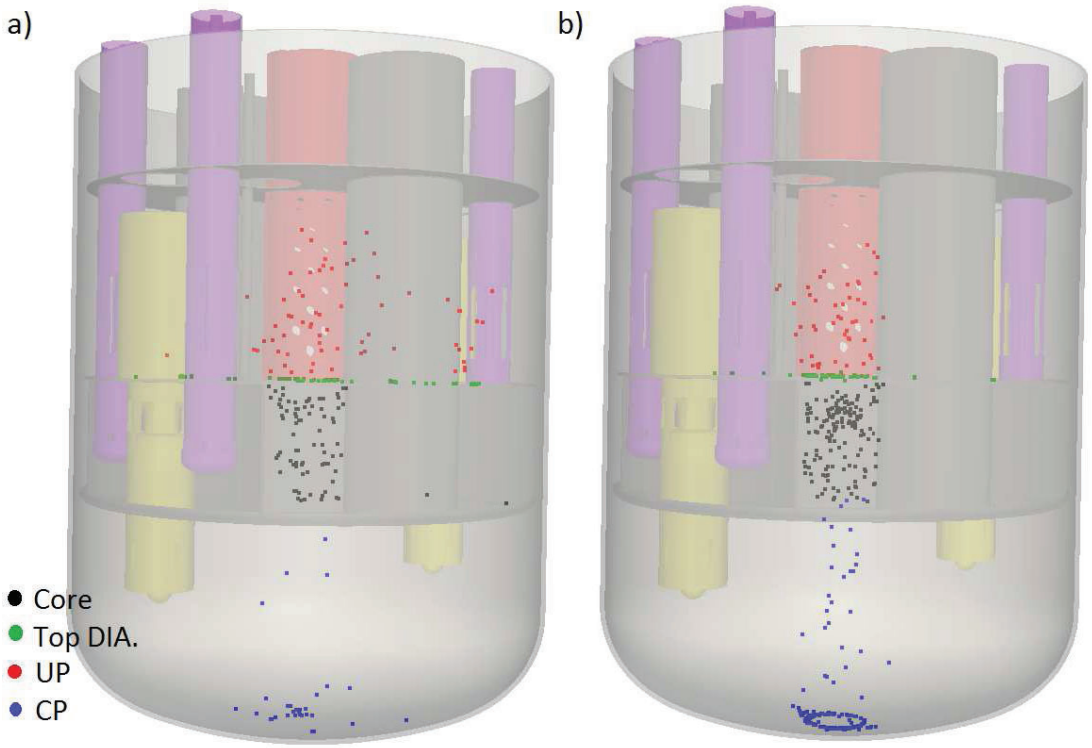

Figure 14. Case 4 – Final particle positions with continuous tracking a) 3 % CP b) 1 % CP

To conclude, considering that an important quantity of particles goes through the core, a more elaborate modeling of the core is required to simulate this case accurately in natural convection. Moreover, large particles that drop through the core have a high chance of getting stuck inside the core, thus preventing them from dropping to the bottom; a detailed model of this area would be required to correctly assess this risk. However, these first results indicate that there is a strong risk of particle accumulation on the top diaphragm plate and at the bottom of the vessel.

4. CONCLUSIONS

The aim of this work has been to study the long term dispersion of fuel particles inside the MYRRHA reactor. A summary of the results obtained in forced and natural convection is proposed in Fig. 15 and 16 respectively. For each case, the proportion of particles that reach the various zones is represented. The distributions obtained in nominal conditions show that for densities as low as 60 % of TD, free-surface accumulations should be expected. The cases where particles re-enter the core are mainly restricted to small diameters such that the actual risk of core damage is limited. Nevertheless, the heaviest particles represent an additional threat of fuel accumulation in localized areas of the top diaphragm plate.

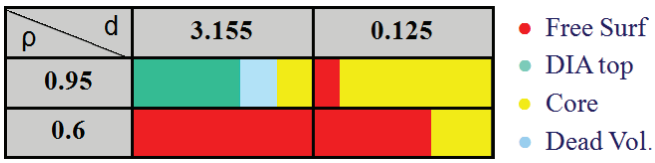

Figure 15. Summary of the fuel dispersion results obtained in nominal conditions

In natural convection, the free-surface accumulations dominate the cases at low density, with a situation where the largest particles remain stuck inside the barrel. The heaviest particles are again partly dropping on top of the diaphragm plate but also straight down to the bottom of the vessel, especially in the case of a normal reactor shutdown (1 % CP).

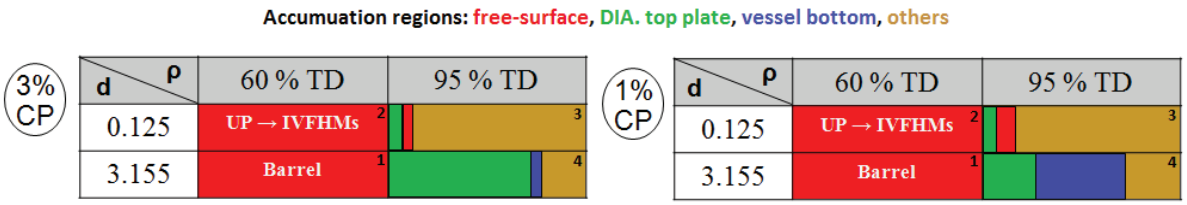

Figure 16. Summary of the fuel dispersion results obtained in natural convection

In this flow regime, the flow is not energetic enough to prevent the densest particles from re-entering the core region. Furthermore, this phenomenon is enhanced by the inflow observed through the first row of barrel holes, which can bring back particles that had passed to the UP into the barrel region.
In general, an accurate modeling of particle behavior throughout the core region would require a more detailed description of the core. Indeed, taking into account the actual geometry would be more representative of potential fuel bundle blockage. VKI will focus on this problematic in the frame of future European collaborations such as the MYRTE project.

AKNOWLEDGMENTS

This work has been performed in collaboration with the SCK•CEN and is funded through the DEMOCRITOS research contract financed by BELSPO (Belgian Science Policy Office) and the European SEARCH FP7 project (Contract number: 295736).

REFERENCES

1. http://myrrha.sckcen.be/
2. L. Koloszar et al., “CFD simulation of the thermohydraulics of the MYRRHA reactor,” THINS 2014 International Workshop, Modena, Italy, January 20-22, 2014.
3. S. Buckingham et al., “Lagrangian tracking of fuel particles in the MYRRHA reactor,” THINS 2014 International Workshop, Modena, Italy, January 20-22, 2014.
4. P. Raynaud, “Fuel fragmentation, relocation, and dispersal during the loss-of-coolant accident,” NUREG-2121, U.S. NRC, 2012.
5. Handbook on Lead-Bismuth Eutectic Alloy and Lead Properties, Nuclear Energy Agency 2007 Edition, http://www.nea.fr/html/science/reports/2007/nea6195-handbook.html